REPORT DOCUMENTATION PAGE

AFRL-SR-BL-TR-01-

0189

1. AGENCY USE ONLY (Leave blank)

2. REPORT DATE
2/28/01

3. REPORT TYPE AND DATES COVERED
Final Technical 10/1/94-9/30/96 1/15/97

4. TITLE AND SUBTITLE
Computational Simulation of Unsteady, Viscous, Hypersonic Flow about Flight Vehicles with Store Separation

5. FUNDING NUMBERS
F49620-95-1-0020

6. AUTHOR(S)
David L. Marcum

7. PERFORMING ORGANIZATION NAME(S) AND ADDRESS(ES)
Mississippi State University
P.O. Box 6156
Mississippi State, MS 39762

8. PERFORMING ORGANIZATION REPORT NUMBER

9. SPONSORING/MONITORING AGENCY NAME(S) AND ADDRESS(ES)
Air Force Office of Scientific Research
801 North Randolph Street, Room 732
Arlington, VA 22203-1977

10. SPONSORING/MONITORING AGENCY REPORT NUMBER

11. SUPPLEMENTARY NOTES
The views, opinions and/or findings contained in this report are those of the author and should not be construed as an official Air Force position, policy, or decision, unless so designated by other documentation.

12a. DISTRIBUTION/AVAILABILITY STATEMENT
Approved for public release; distribution unlimited.

12b. DISTRIBUTION CODE

13. ABSTRACT (Maximum 200 words)

This project describes a research project to develop a computational capability to accurately and efficiently simulate unsteady, three-dimensional, hypersonic, viscous flow fields about realistic flight vehicle configurations with separating stores and/or components. Unstructured grid technology with an advanced implicit high-resolution flow field solution algorithm is utilized as the basis for this computational capability. The solution algorithm uses an implicit Newton-relaxation scheme with approximate LU factorization and Roe flux-difference splitting. A new unstructured grid generation procedure labeled Advancing-Front/Local-Reconnection (AFLR) was developed that significantly improves the state-of-the-art. This procedure uses an iterative point placement scheme. New points are generated using advancing-front type point placement and the connectivity is optimized with iterative local-reconnection. The combined efficiency, quality, and robustness for AFLR are a substantial improvement over existing techniques. Unsteady and steady flow fields about complex flight vehicles with separating components were simulated to demonstrate, test, and validate the overall computational procedure.

14. SUBJECT TERMS
computational fluid dynamics, unstructured grid generation

15. NUMBER OF PAGES
24

16. PRICE CODE

17. SECURITY CLASSIFICATION OF REPORT	18. SECURITY CLASSIFICATION OF THIS PAGE	19. SECURITY CLASSIFICATION OF ABSTRACT	20. LIMITATION OF ABSTRACT
UNCLASSIFIED	UNCLASSIFIED	UNCLASSIFIED	UL

NSN 7540-01-280-5500

Standard Form 298 (Rev. 2-89)
Prescribed by ANSI Std. Z39-18

Final Report

AFOSR Grant No. F49620-95-1-0020

COMPUTATIONAL SIMULATION OF UNSTEADY, VISCOUS, HYPERSONIC FLOW ABOUT FLIGHT VEHICLES WITH STORE SEPARATION

Mississippi State University
NSF Engineering Research Center for Computational Field Simulation
P.O. Box 6176
Mississippi State, Mississippi 39762

TABLE OF CONTENTS

1. ABSTRACT	2
2. INTRODUCTION	3
3. UNSTRUCTURED GRID GENERATION	5
4. SOLUTION ALGORITHM	8
5. RESULTS	14
6. REFERENCES	21

1. ABSTRACT

This report describes a research project to develop a computational capability to accurately and efficiently simulate unsteady, three-dimensional, hypersonic, viscous flow fields about realistic flight vehicle configurations with separating stores and/or components. Unstructured grid technology with an advanced implicit high-resolution flow field solution algorithm is utilized as the basis for this computational capability. The solution algorithm uses an implicit Newton-relaxation scheme with approximate LU factorization and Roe flux-difference splitting. A new unstructured grid generation procedure labeled Advancing-Front/Local-Reconnection (AFLR) was developed that significantly improves the state-of-the-art. This procedure uses an iterative point placement scheme. New points are generated using advancing-front type point placement and the connectivity is optimized with iterative local-reconnection. The combined efficiency, quality, and robustness for AFLR are a substantial improvement over existing techniques. Unsteady and steady flow fields about complex flight vehicles with separating components were simulated to demonstrate, test, and validate the overall computational procedure.

2. INTRODUCTION

Recent advances in solution algorithms, grid generation, and computer architecture have made it possible to simulate flow fields about increasingly complex flight vehicles using computational fluid dynamics (CFD). However, there is still a significant difference between reality and the overall complexity of the simulations. Computational models of flight vehicles that are often called complex or complete are in actuality, simplified approximations to the real vehicle. Simulation of unsteady, viscous flow fields about vehicles with real operating conditions, such as maneuvering vehicles, varying engine conditions, moving components, and/or separating stores, are typically considered too demanding for current technology. The underlying fluid mechanics of such flow fields is not well understood, and computational simulation could provide significant insight. There is real need for a capability to simulate complex flow fields about flight vehicles with realistic geometry and operating conditions. This research project addresses this need for the specific case of flight vehicles with separating stores, which is of importance to the Air Force and the aerospace industry. Computational tools have been developed under this grant for the purpose of investigating and gaining new knowledge of the fluid dynamics involved in such cases. These tools are also directly applicable to a wide variety of problems of interest to the Air Force and industry other than store separation cases.

The objective of this research project was to develop computational tools for simulation of unsteady, three-dimensional, hypersonic, viscous flow fields about realistic flight vehicle configurations with separating stores and/or components such as that shown in Fig. 2.1. Typical flight vehicles of interest operate at Mach numbers that range from 6 to 15. Unstructured grid technology with an advanced implicit high-resolution flow field solution algorithm was utilized to develop this capability.

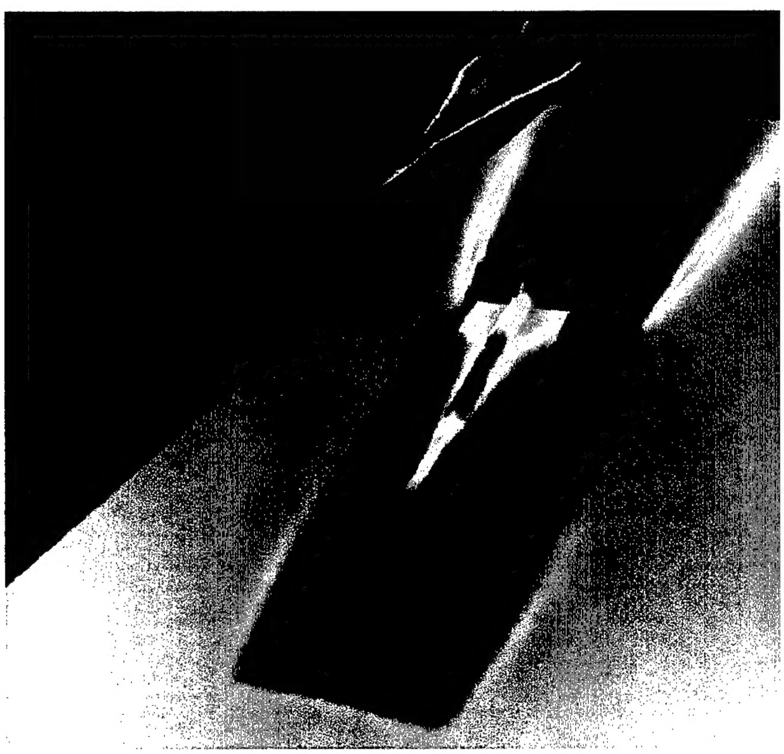

Fig. 2.1. Separating kinetic energy weapon.

Unstructured grid technology is a promising approach offering geometric flexibility for handling of both complex geometry and physics. As such, it can provide a powerful capability, fully meeting the primary objective of accurately and efficiently computing complex unsteady flow fields. There are several researchers that are active in the area of unstructured grid technology. The number of researchers in this area has steadily increased as the technology has been developed into a powerful and useful tool. Several procedures for calculating three-dimensional inviscid flow fields have been developed and successfully applied to complex configurations, examples of which have been presented by Barth [1], Batina [2], Frink et al [3], Jameson et al. [4], Kallinderis et al. [5], Lohner et al [6], Marcum et al. [7], Mavriplis et al. [8], Peraire et al. [9,10], Stoufflet et al. [11], Weatherill et al. [12,13], and others. For calculating viscous flow fields, considerably less work has been published using unstructured grids. In two-dimensions, procedures have been presented with turbulence modeling by Barth [14], Holmes and Connell [15], Mavriplis [16], Pan and Cheng [17], and Rostand [18]. In three-dimensions, a hybrid prismatic procedure has been presented by Nakahashi [19] and fully unstructured procedures have been presented by Chalot et al. [20], Marcum et al [7,21], and Morgan et al [10,22]. The unstructured solution algorithms that have been employed by various researchers include explicit and implicit time discretization, finite-element and finite-volume space discretization, and upwind flux evaluation. While no single approach stands out as clearly superior, an implicit upwind approach appears to offer the most promise for unsteady viscous flow fields.

Solution-adaptive unstructured grid technology developed here at the ERC has been applied to a variety of configurations [12,13,21]. Transonic, inviscid flow fields about wings, commercial aircraft, and military aircraft, such as the F-15 and F-18, have been computed successfully using solution-adapted unstructured grids. Transonic, turbulent flow fields about launch vehicle fore bodies have been calculated using various turbulence models and hybrid unstructured grids. Unsteady, hypersonic, inviscid flow fields about flight vehicles with a separating kinetic-energy weapon and subsequent component separation have been modeled using unstructured grids and trajectories determined from the flow field.

Using an unstructured grid approach, the following components are required to meet the primary objective of this project.

i) A grid generation procedure is required that will efficiently generate and re-generate, without user intervention, fully unstructured grids of high quality which are suitable for viscous flow about complex configurations.

ii) A flow solver is required that will accurately and efficiently compute unsteady viscous flow fields about complex flight vehicle configurations using an unstructured grid.

These components must be developed concurrently and eventually work together as one procedure.

Much of the basic technology required to develop the computational tools for this research work existed at the start of this research work. However, it became clear as the work progressed that existing technology was in some cases not suitable for unsteady applications with complex geometry in relative motion. In particular, state-of-the-art unstructured grid generation procedures based on traditional advancing-front or Delaunay were found to be in need of significant improvements for these applications. Existing procedures simply were not robust enough and either required excessive computational resources or produced grids of low quality

or both. A significant portion of the grant work was focused on solving this problem. As a result the state-of-the-art in unstructured grid generation was significantly enhanced by the development of a new unstructured grid generation procedure [25,26]. This procedure was labeled Advancing-Front/Local-Reconnection (AFLR). It uses an iterative point placement scheme wherein new points are generated using advancing-front type point placement and the connectivity is optimized with iterative local-reconnection. The combined efficiency, quality, and robustness for AFLR are a substantial improvement over existing techniques. As a consequence, the feasibility of unsteady applications with complex moving geometry was significantly enhanced. This advance has also had a significant impact on other application areas. In particular, the AFLR procedure is widely used in the automotive industry for structural, manufacturing, and other applications.

Results were obtained for a variety of static and dynamic store separation and launch vehicle applications. While the scope of the grant did not allow for in-depth validation or extended evaluation of unsteady applications, the results do demonstrate the level of complexity that can be handled using the present approach. They also indicate that additional work is required on improving efficiency. In particular, follow on work should be focused on the implicit solver development in a parallel or distributed processing environment.

In the following sections, additional details on the unstructured grid generation procedure, solution-algorithm, and results are presented.

3. UNSTRUCTURED GRID GENERATION

The most significant accomplishment for this research project is the successful development of the Advancing-Front/Local-Reconnection (AFLR) unstructured grid generation procedure [25,26]. Unstructured grid generation procedures for triangular and tetrahedral elements in use now are typically based on an octree [27], advancing-front [28,29], or Delaunay [30-33] approach. Unfortunately, with these procedures either efficiency or grid quality is relatively poor, especially in three-dimensions. Alternative approaches can be developed using automatic point insertion with a suitable point placement and local-reconnection to optimize the connectivity. This approach has been taken by the Principal Investigator to develop a very efficient local reconnection procedure using advancing-front point placement for generation of triangular or tetrahedral element grids named AFLR. This method has been extended for generation of high-aspect ratio elements using advancing-normal point placement. It has also been extended for generation of structured element types (quadrilateral, prism, hexahedral, etc.) using advancing-point point placement. High-quality isotropic and high-aspect ratio element unstructured grids have been efficiently generated using this method for a variety of geometrically complex configurations. Various point placement strategies and connectivity criteria can readily be incorporated. The flexibility and generality inherent in this approach make it ideally suited to a wide variety of computational field simulation applications.

The AFLR procedure is of significance to all disciplines of computational field simulation. It provides a substantial increase in efficiency and grid quality. In most cases, the increased grid quality improves the solution algorithm efficiency and accuracy. User-time required to generate a grid for a realistic configuration has also been reduced by minimizing required user-input, improving robustness, and increasing computational efficiency. For the current project, this grid generation technology is essential for the resulting research capability to be useable for the intended complex unsteady applications. This technology is also applicable to many areas of interest to the Air Force. Essentially, any computational field simulation application with complex geometry can benefit. This technology has been and transferred to the aerospace and automotive industry. It is currently in use for a variety of disciplines, including, computational fluid dynamics, computational structural analysis, computational electro-magnetics and computational heat-transfer. Applications range from military aircraft to automotive interior heating and cooling.

The triangular/tetrahedral grid generation procedure used in AFLR is a combination of automatic point creation, advancing-front, point and normal point placement and connectivity optimization schemes. A valid grid is maintained throughout the grid generation process. This provides a framework for implementing efficient local search operations using a simple data structure. It also provides a means for smoothly distributing the desired point spacing in the field using a point distribution function. This function is propagated through the field by interpolation from the boundary point spacing or by specified growth normal to the boundaries. Points are generated using either advancing-front type placement for isotropic elements, advancing-point type placement for isotropic right angle elements, or advancing-normal type point placement for right angle high-aspect ratio elements. The connectivity for new points is initially obtained from direct subdivision and then improved by iteratively using local-reconnection subject to a quality criterion. A min-max type (minimize the maximum angle) criterion is used. The overall procedure is applied repetitively until a complete field grid is obtained.

High-quality isotropic and high-aspect ratio element two- and three-dimensional grids have been efficiently generated about geometrically complex configurations using this procedure. Required CPU times for this method on various computers are shown in Fig. 2.1. The CPU times shown include all steps in the procedure including I/O and are for generation of isotropic elements about a variety of configurations. Generation times for grids with high-aspect ratio elements are slightly lower. As shown the required CPU times for generating field grids about realistic configurations is reasonable and are a substantial improvement over other methods. Complete details of the AFLR procedure are presented in Refs. 25 and 26.

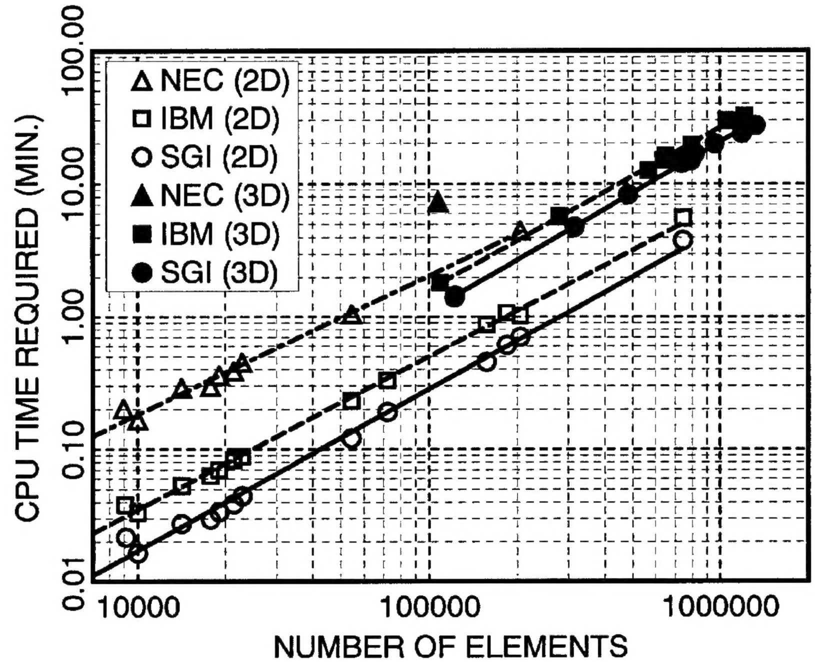

Fig. 2.1. CPU time required. NEC denotes NEC Ultralite VERSA 486SL33 laptop, IBM denotes IBM R6000 550E, and SGI denotes SGI 150 Mhz Indigo.

4. SOLUTION ALGORITHM

A general data structure that is independent of the element type is required for the flow solver. A successful data structure must be invariant to the global structure of the grid. It also should exploit, wherever possible, local structure at the element level. In our approach, a local edge based data structure is used. Two data points are attached to each edge. The edge data points are equivalent to locations i and $i+1$ of a structured grid. Associated with each edge is an area and a volume. Linking edges to closely aligned edge neighbors to form a local structured connectivity can also expand this data structure. This connectivity is equivalent to locations $i-1$, i, $i+1$, $i+2$ of a structured grid as illustrated in Fig. 4.1. Ideally, the connected edges should form a very smooth line. However, for a typical grid with varying element volumes or types, there will be some connected edges that do not form a smooth line. Based on results obtained with such connections, this does not create any numerical difficulties. The local structured edge connectivity allows direct implementation of many high-resolution upwind schemes developed for structured grids. The high-order terms in such schemes can be obtained directly using the aligned neighboring edges or indirectly from gradients of the flow properties determined at both edge data points. The gradient approach offers potentially more accuracy for non-aligned cases at the expense of more computational work. Both approaches have been implemented.

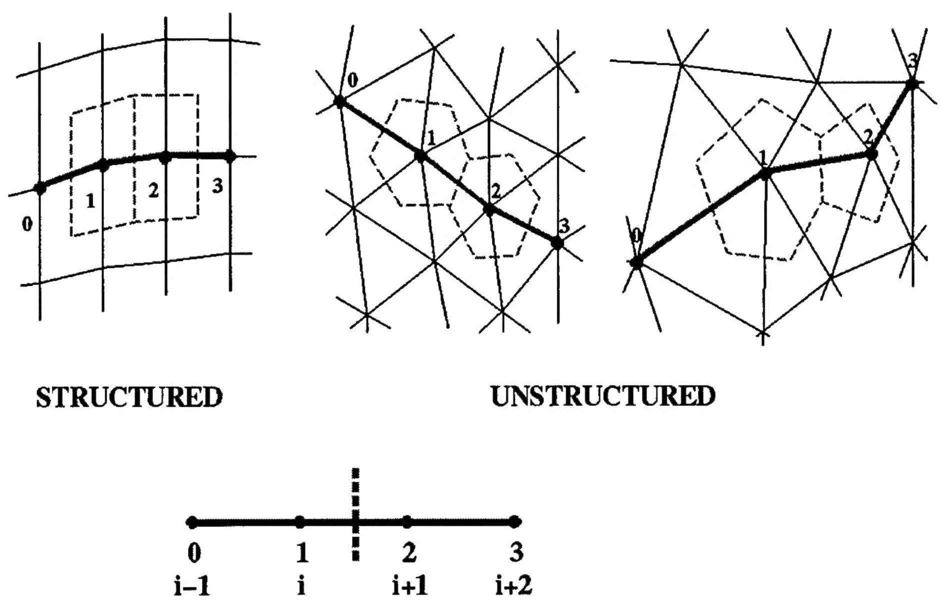

Figure 4.1. Local edge based data structure.

The edge based data structure can be used with either vertex based or centroid based solution algorithms. Within the flow solver, the solution algorithm for either scheme is identical. Only the initial geometric setup and boundary condition implementation differ. The edge data structure is extracted from the basic grid information for each element. The contribution from an element to the total area and volume for an edge is dependent upon the element type. For vertex-based data, the two edge data points along with the element centroid, the face centroids of the two element faces attached to the edge, and the midpoint of the edge define the element area and volume contributions as shown in Fig. 4.2. For centroid based data, the element area and volume contributions are defined by the two edge data points along with the element centroid and the

element face points of the face attached to the edge as shown in Fig. 4.3. The procedures developed for this project were designed to be very general so that they can be used with varying topology and element type and that they can be efficiently used on a variety of computer architectures. The edge data structure can also be used with a grid decomposed into sub domains for parallel or distributed processing.

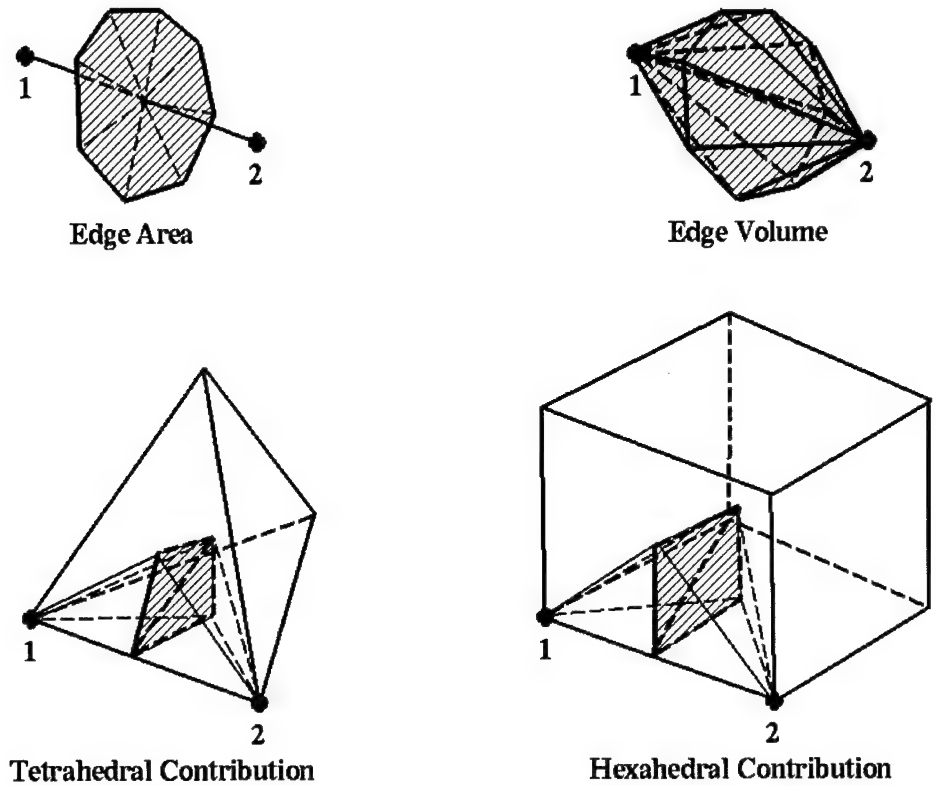

Fig. 4.2. Edge area and volume contributions for vertex based data.

An accurate and efficient solution algorithm is required to meet the primary objective of this project. The algorithm must effectively eliminate the CFL restriction imposed by high aspect ratio elements within shear layers. It must also accurately simulate the flow field with varying high gradient features, such as shock waves, contact discontinuities, rapid expansions, shear layers, etc. The solution algorithm developed for this project is based upon the structured algorithm developed by Whitfield et al [23,24] that is an implicit Newton-relaxation scheme with an approximate LU factorization and Roe flux-difference splitting. Implicit algorithms with Roe flux-difference splitting have been successfully developed by others for single element type unstructured grids. These include, the inviscid three-dimensional procedure developed by Batina [2] which includes an implicit Gauss-Siedel scheme and the viscous two-dimensional procedure developed by Pan and Cheng [16] which includes an implicit approximate LU factorization scheme.

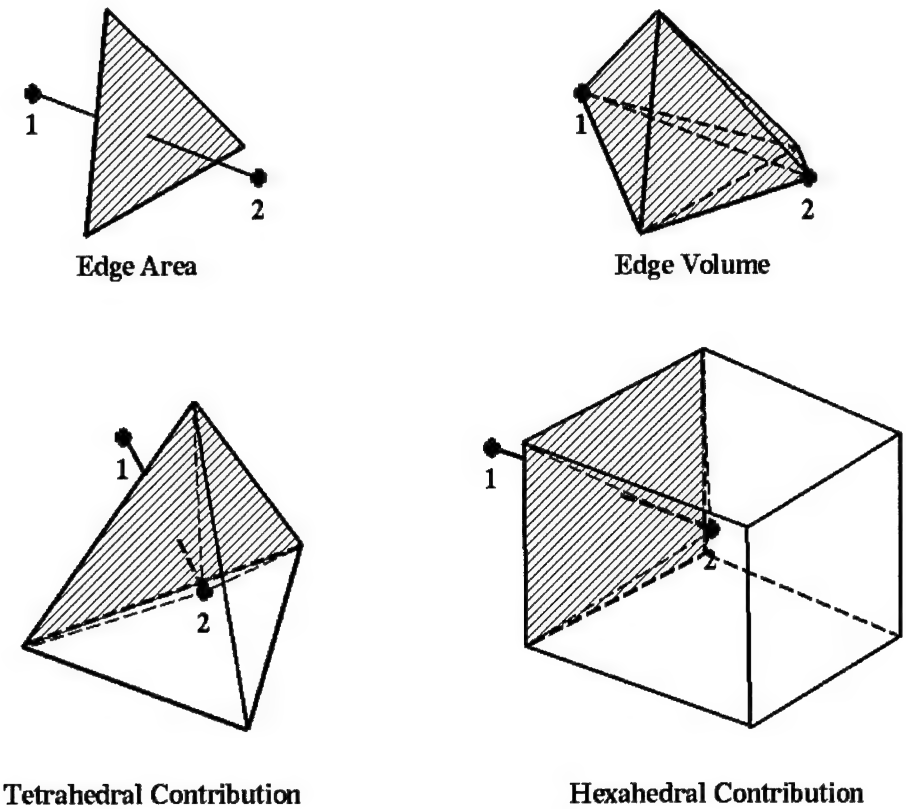

Fig. 4.3. Edge area and volume contributions for centroid based data.

Given the previously described data structure, the governing equations can easily be discretized in space using a finite volume approach. Discretization of the Reynolds-Averaged Navier-Stokes equations expressed in integral form results in a formulation that involves summation of fluxes over a control volume. The net flux or residual can be approximated by summing for a given solution point the average flux through the area associated with each edge connected to the point. A dissipative term can be added to the inviscid flux vector for stability and capturing discontinuities. Using Roe flux-difference splitting [34], the dissipative term is obtained from the sum of the difference in the flux vector along each characteristic curve associated with each eigenvalue of a one-dimensional system aligned with the edge. High-order schemes can be obtained by using a Taylor series expansion to extrapolate the primitive variables. This requires gradients of the solution variables which can be obtained using the previously described local structured edge connectivity, directed gradients evaluated at the end points of the basic edge, or a least-squares approach [35]. The least-squares approach appears to offer the best robustness. Limiting is required with the high-order inviscid flux vector to prevent the creation of local extrema when variables are extrapolated. The elimination of local extrema is required to preserve monotonicity and to avoid the development of spurious oscillations near solution discontinuities. The limiter function is applied to the Taylor's series expansion. Two different limiters are currently available in the flow solver. They are: (i) Barth's limiter [36] and (ii) Venkatakrishnan's limiter [37]. During the course of development of the flow solver, it was observed that Venkatakrishnan's limiter can produce varying pressure distributions depending on the choice of the thresholding parameter. At present, the Barth limiter is preferred with the present technology. However, further investigation is required.

The gradients required for the viscous flux computations are calculated using a Green's theorem approach modified with a directed gradient. Green's theorem in standard form is used to compute the gradient at each node. Then an average gradient is obtained for each edge. However, this produces a lower accuracy then its structured equivalent. This is due to the averaging process that produces a second-order error term that is based on twice the local spacing (2h rather than h). A directed gradient correction can be used to improve this accuracy. In this approach the component of the average gradient tangent to the edge is replaced with a directed gradient based on the difference between the solution variables at the two edge nodes. This component has an error term four times as accurate as the simple average. This scheme also has the advantage that it can be used directly with elements of any type, such as tetrahedral, pentahedral, hexahedral, etc. A standard Green's theorem approach requires differing formulations with greater complexity for each element type.

An implicit time discretization is used in the solution algorithm proposed for this project. A Newton-relaxation scheme with approximate LU factorization is used to solve the implicit discretized equations. In this approach, Newton's method is used to determine a solution vector that satisfies the discretized unsteady equations. The flux-Jacobians required for Newton's method need not be exact and can be approximated without any loss in accuracy. Efficiency can be improved by using flux-Jacobians from a flux splitting scheme rather than those from the flux-difference splitting scheme used to determine the residual [23,24]. The system of equations that result from the Newton-linearization is solved using a modified two-pass approximate LU factorization scheme. These equations need not be solved exactly and can be solved approximately without any degradation in accuracy. This implicit approach has been used successfully with structured grids for steady and unsteady viscous flow fields at the ERC [23,24]. Time steps corresponding to CFL values in the thousands have been obtained with structured grids on fairly complex configurations. Eliminating the CFL restriction imposed by high-aspect ratio elements in shear layers is essential for unsteady viscous flow calculations to be feasible.

Results with unstructured grids indicate that the implicit scheme is invariant to the global structure of the grid provided a suitable reordering scheme is used. A reordering that results in vertices ordered with some relation to their location in space appears to be adequate. Such a reordering can be readily obtained for unstructured grids. Other than the required reordering, the implicit algorithm is essentially identical between the structured and unstructured versions.

The finite volume scheme described here has been used successfully with structured grids and more recently with unstructured grids. The implementation is done nearly identical to that for the structured case. The primary difference is that with structured grids the high-order terms are usually obtained using the points $i-1$ and $i+2$ adjacent to an edge containing points i and $i+1$ rather than directed gradients or least-squares. Similarities with structured grids allow us to utilize the significant expertise in structured solution algorithms that is available at the ERC.

A turbulence model is required to obtain the turbulent viscosity coefficient. For the present research work, the turbulent viscosity is computed using a simplified form of the Spalart–Allmaras one–equation turbulence model [38]. This model is a second-order partial differential equation that is solved de-coupled from the governing equations. Fully turbulent flow is assumed and the turbulence transition terms are neglected to produce a slightly simplified form of the turbulence model.

The trajectories of moving bodies are determined from a time-integration of the aerodynamic forces acting on the bodies. A full six degree of freedom kinematics model with translation and rotation is implemented. The time-integration of the kinematics equations is explicit and is solved de-coupled from the flow field solver. Force and moments are obtained using a surface integration of the flow field.

A deforming grid is used in the present work. To account for grid motion, the governing equations are modified by adding a grid velocity term to the convective flux terms for mass, momentum, and energy. Either modifying the time derivative term or adding a separate grid conservation law can account for the effects of a time-dependent element volume. In the present work a grid conservation law is used.

As the grid deforms the local element quality typically degrades. Eventually the grid must be regenerated to prevent the solver performance from being impacted. Deformation and re-generation are done locally in prescribed regions for optimal performance. Surrounding each body is a region of elements that move rigidly with the body as shown in Fig. 4.4. Between bodies, elements deform when there is relative motion (also shown in Fig. 4.4). Periodically, a new grid is generated in the deforming region to minimize distortion of deforming elements. This grid movement scheme is suitable for both viscous and inviscid flow fields. In the viscous case, the rigid region is essential, as the required high aspect ratio elements would distort significantly with only minimal movement. Actual movement of the grid is related to the distance from a moving body. Using a "layered" approach this can be determined directly without iteration from the motion of the bodies. Topological "layers" are used to define the deforming and rigid regions as shown in Fig. 4.5. A coefficient based on the distance from a moving body is used to determine the deformation. This coefficient varies from zero (rigid body motion) at the moving body surface to one (no motion) away from the body. The grid deforms locally if the coefficient is between zero and one.

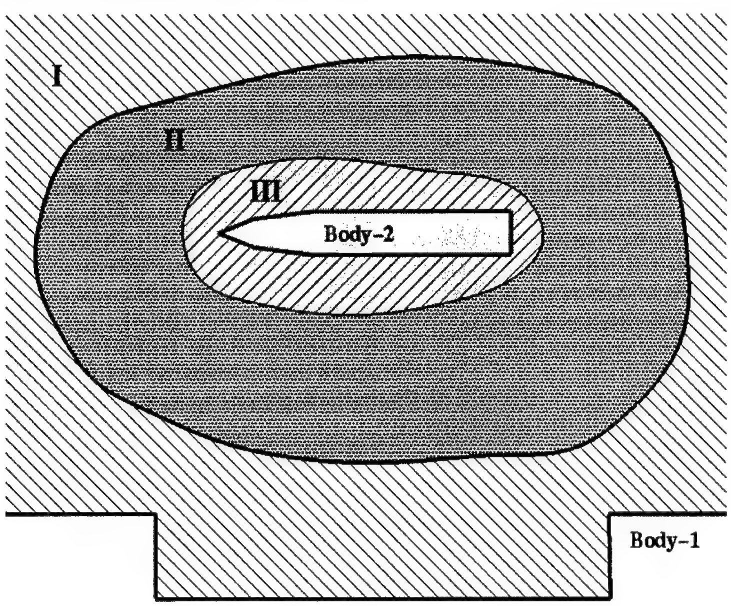

I Grid rigidly attached to Body-1
II Grid deforms when there is relative motion
III Grid rigidly attached to Body-2

Fig. 4.4. Rigid and deforming regions for relative motion applications.

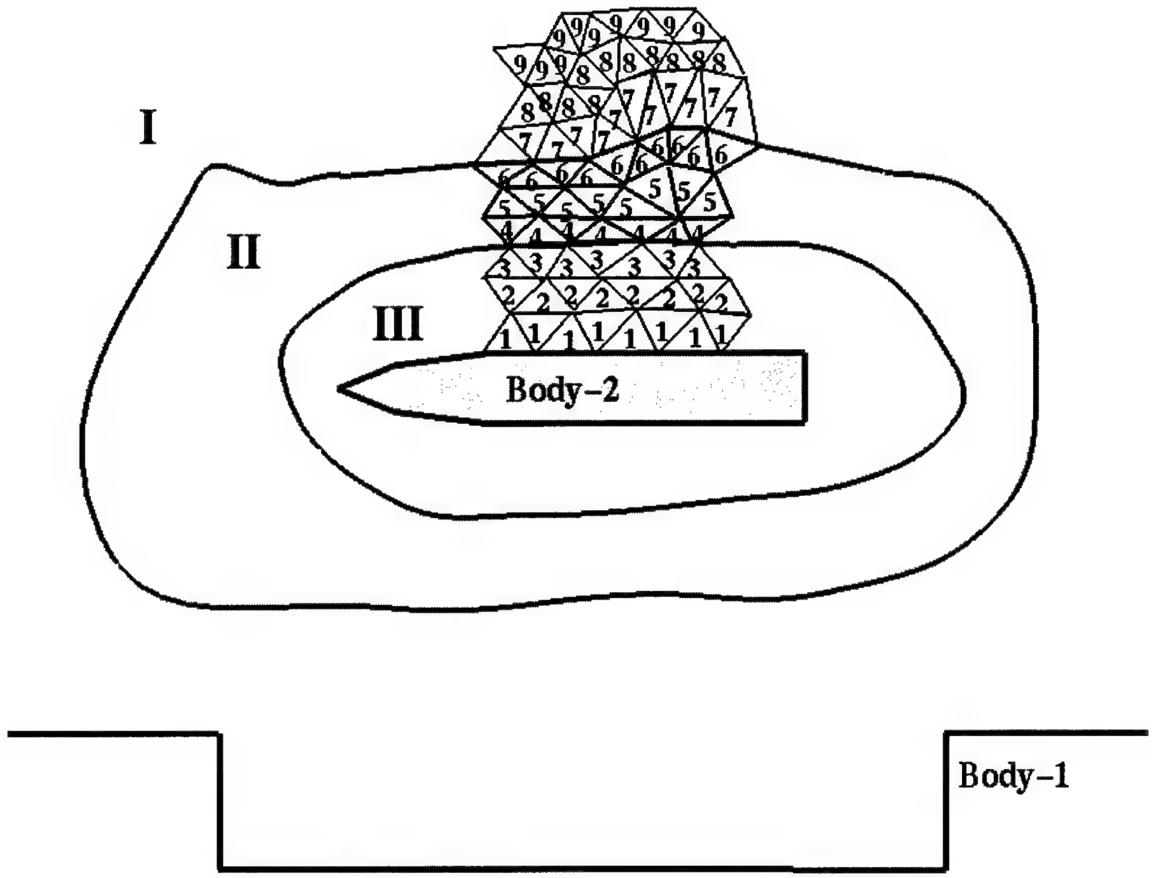

I 1, 2, 3 $\beta = 1, 1, 1$
II 4, 5, 6 $\beta = 0.75, 0.5, 0.25$
III 7, 8, 9 $\beta = 0, 0, 0$

Fig. 4.5. Use of layers for grid deformation.

5. RESULTS

Selected results are presented here to demonstrate the basic capabilities of the tools developed for this research project. One example that includes multiple simulations is shown in Fig. 5.1. For this configuration the main hypersonic vehicle contains a cavity on the top surface from which a much smaller kinetic energy weapon (KEW) vehicle is separated. As shown in Fig. 5.2 the KEW vehicle consists of an embedded kinetic energy weapon surrounded by two shrouds and an engine section. In the overall simulation the flow about the main vehicle is simulated first to get the flow field near the cavity. Next the domain is reduced to the cavity region and KEW vehicle only as shown in Figs. 5.3, 5.4 and 5.5. The flow field from the initial simulation is then used as a boundary condition for the unsteady simulation of the separating KEW vehicle. The main vehicle is moving at Mach 8 and the store is ejected with an initial velocity of 30 m/s. Mach number contours are shown in Figs 5.6, 5.7 and 5.8 at various stages of the simulation. Pressure contours for a simulation of the final shroud separation are shown in Fig. 5.9.

The present technology has also been applied extensively to launch vehicle applications. A generic Delta configuration was simulated during separation of the strap-on boosters at a Mach number of 2.1. There are a total of nine strap-on boosters surrounding the main vehicle and every other one is separating. Pressure contours for a single separation location are shown in Figs. 5.10, 5.11 and 5.12.

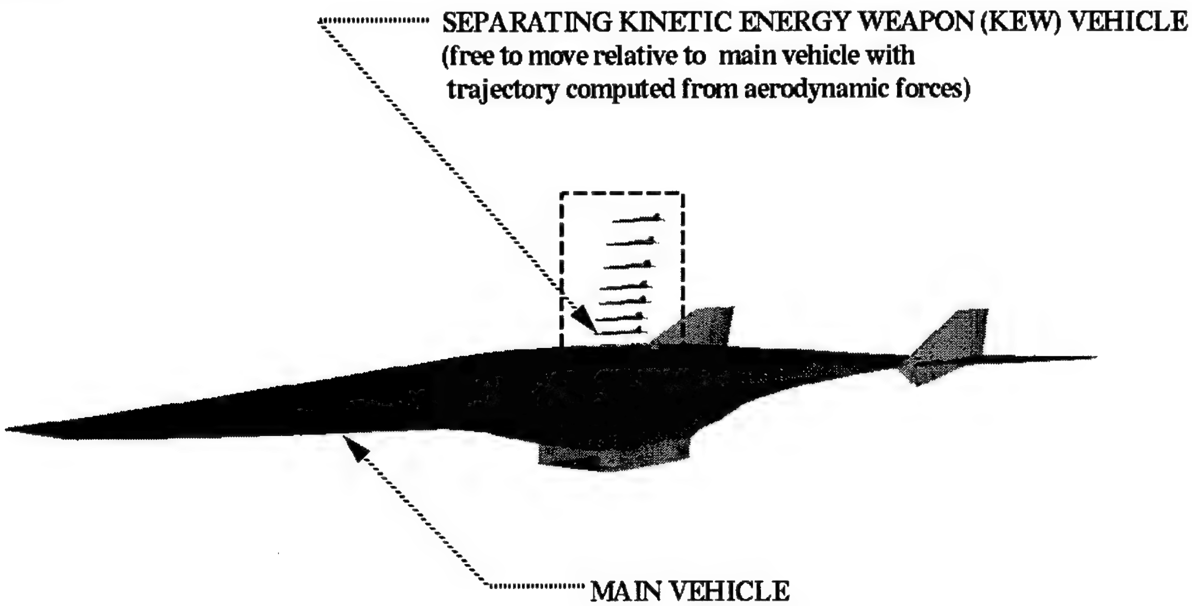

Fig. 5.1. Generic hypersonic vehicle with a separating kinetic energy weapon.

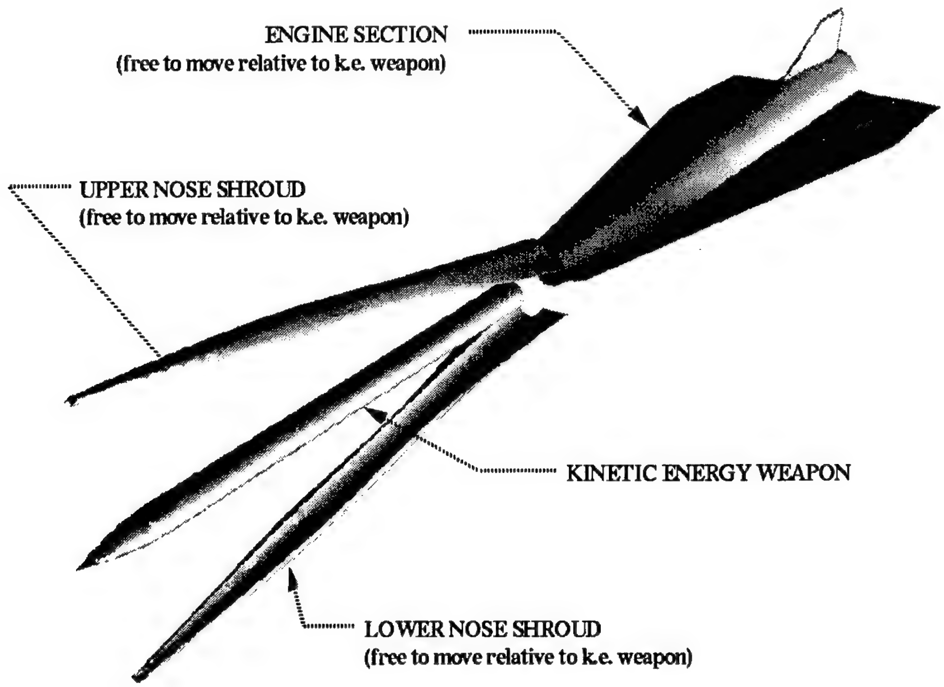

Fig. 5.2. Generic kinetic energy weapon.

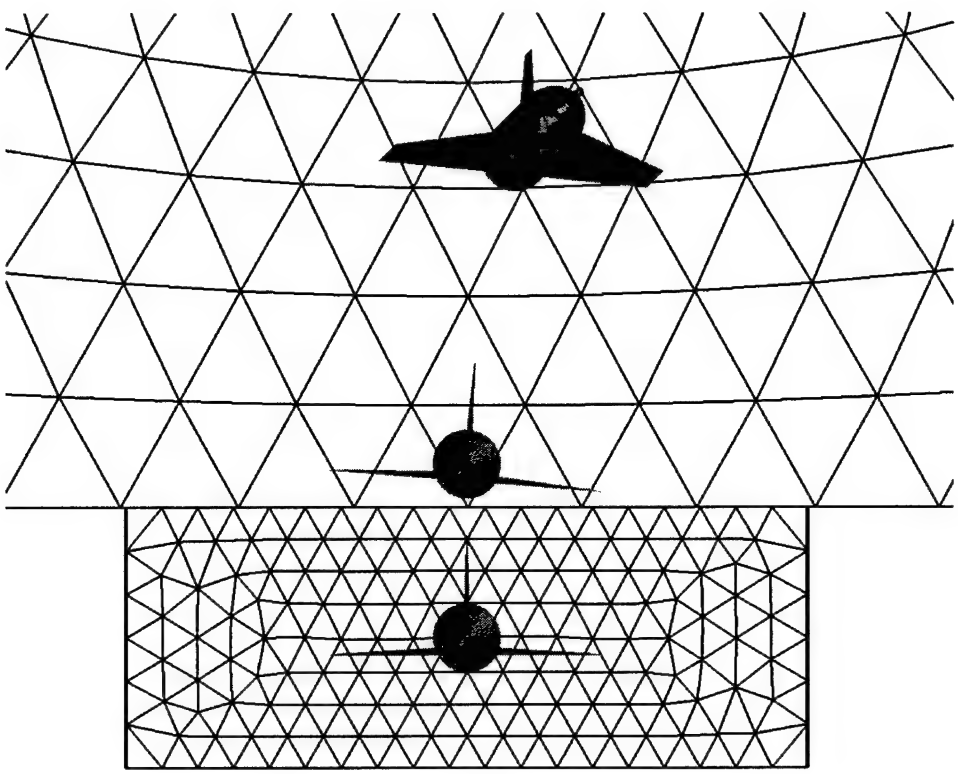

Fig. 5.3. Forward view of separating KEW vehicle at three different positions.

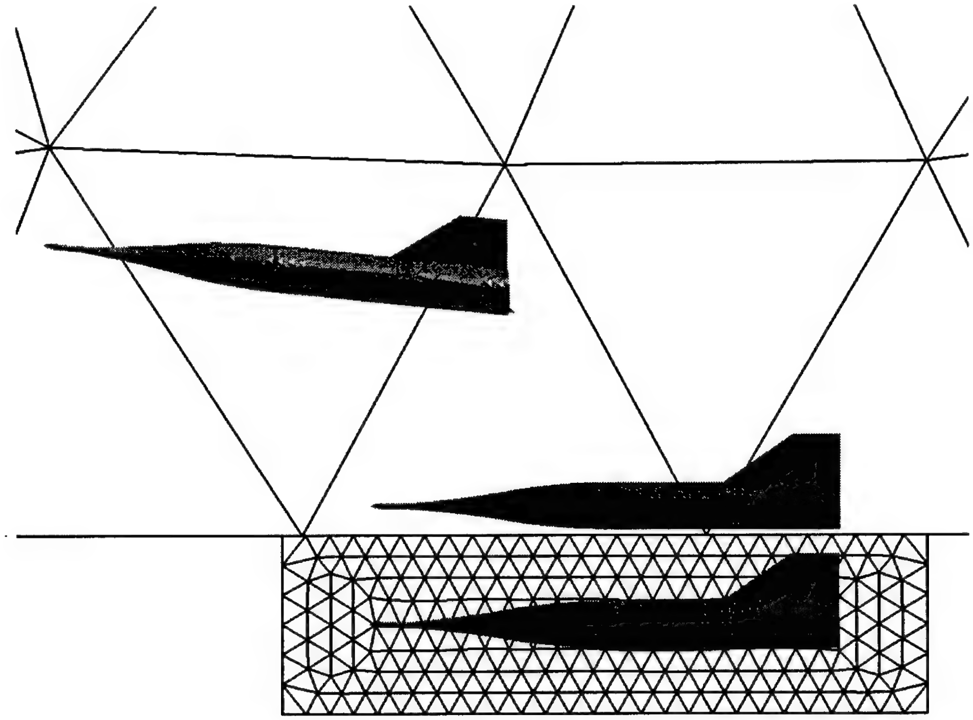

Fig. 5.4. Side view of separating KEW vehicle at three different positions.

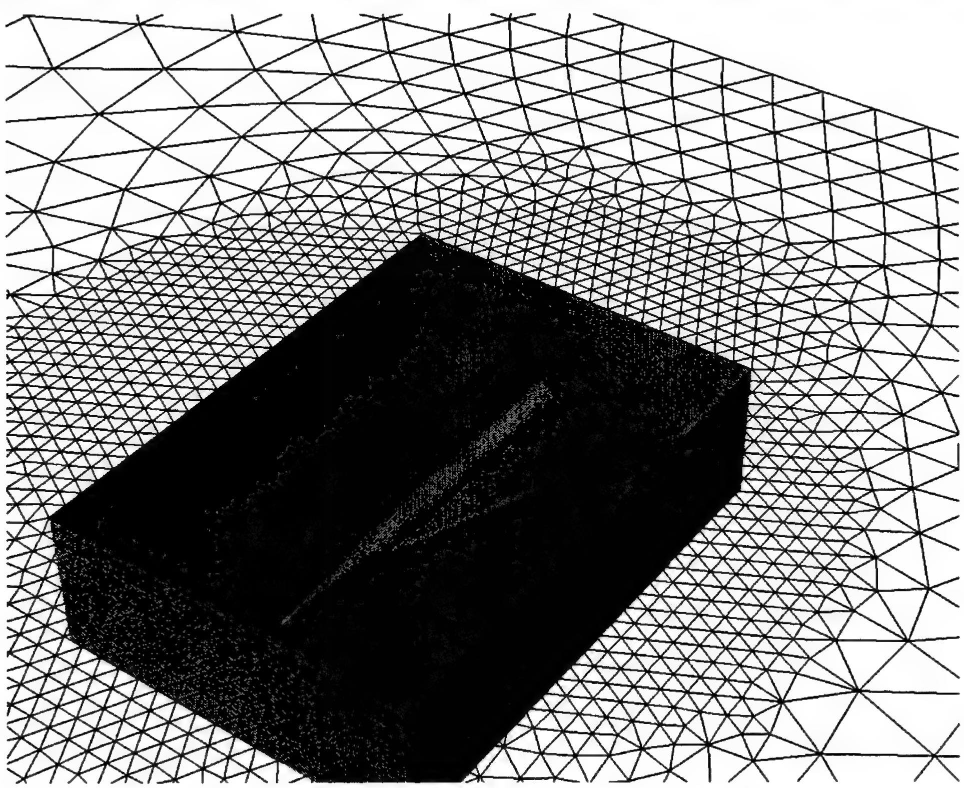

Fig. 5.5. Separating KEW vehicle in main vehicle cavity.

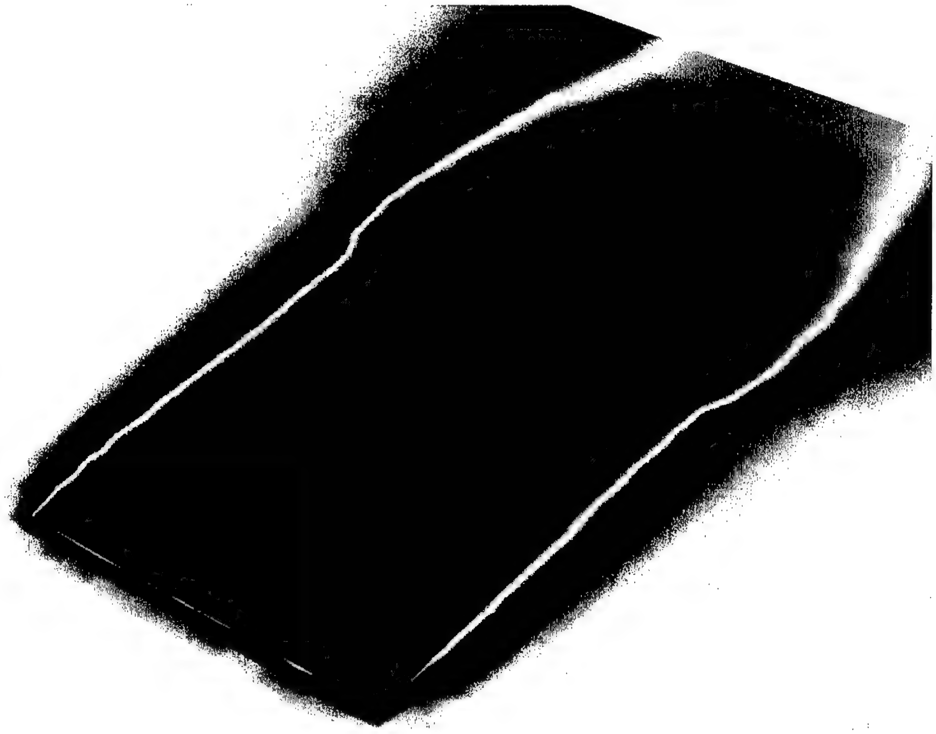

Fig. 5.6. Mach number contours on main vehicle surface.

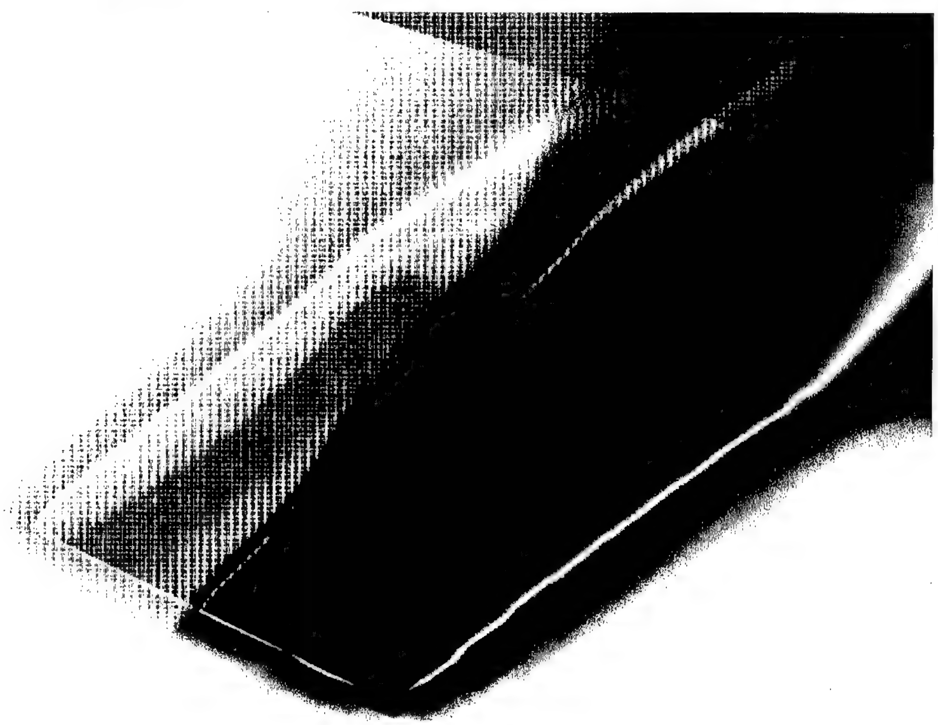

Fig. 5.7. Mach number contours on mid-plane and main vehicle surface when KEW is just leaving main vehicle cavity.

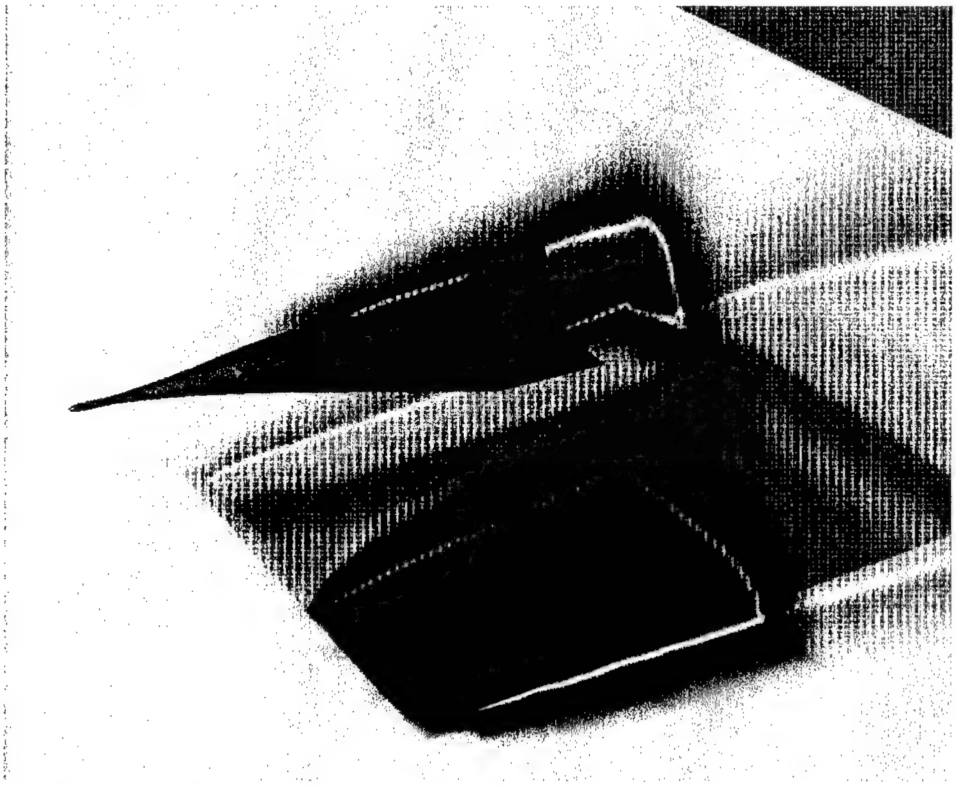

Fig. 5.8. Mach number contours on mid-plane and main vehicle surface after KEW has left main vehicle cavity and KEW motor has ignited.

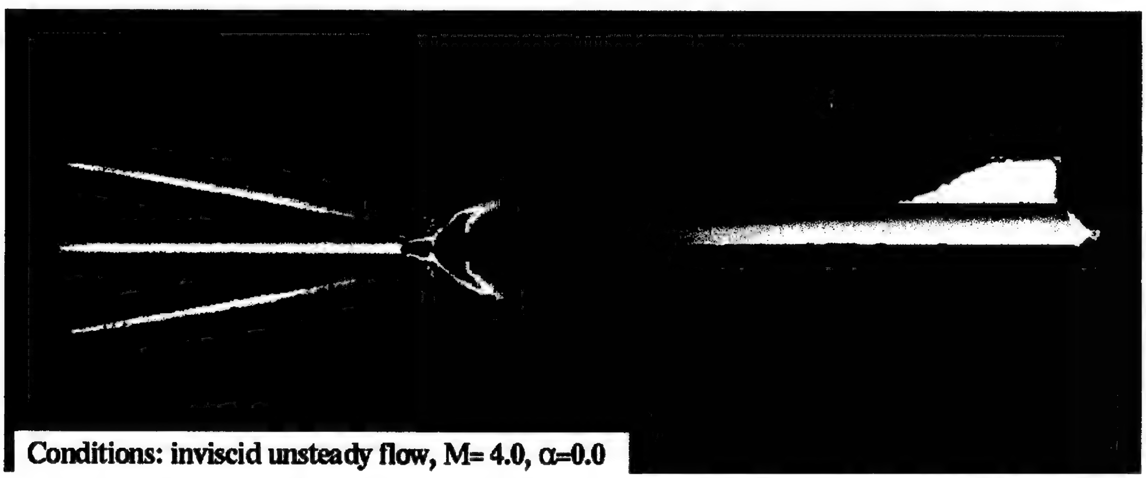

Fig. 5.9. Pressure contours during shroud separation from the KEW.

Fig. 5.10 Delta launch vehicle pressure contours.

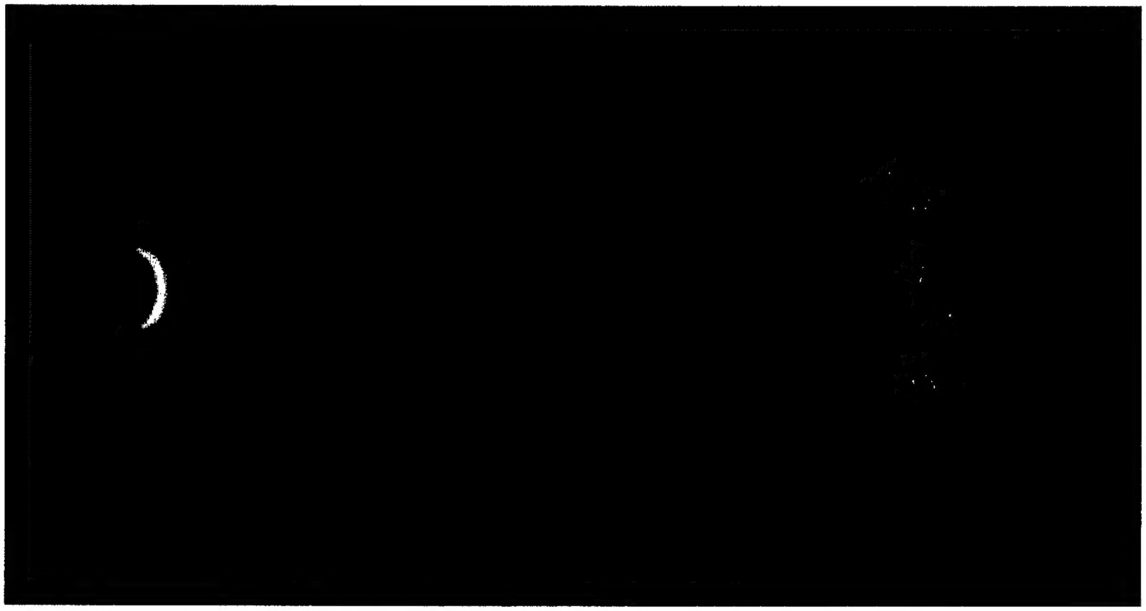

Fig. 5.11 Forward view of Delta launch vehicle pressure contours.

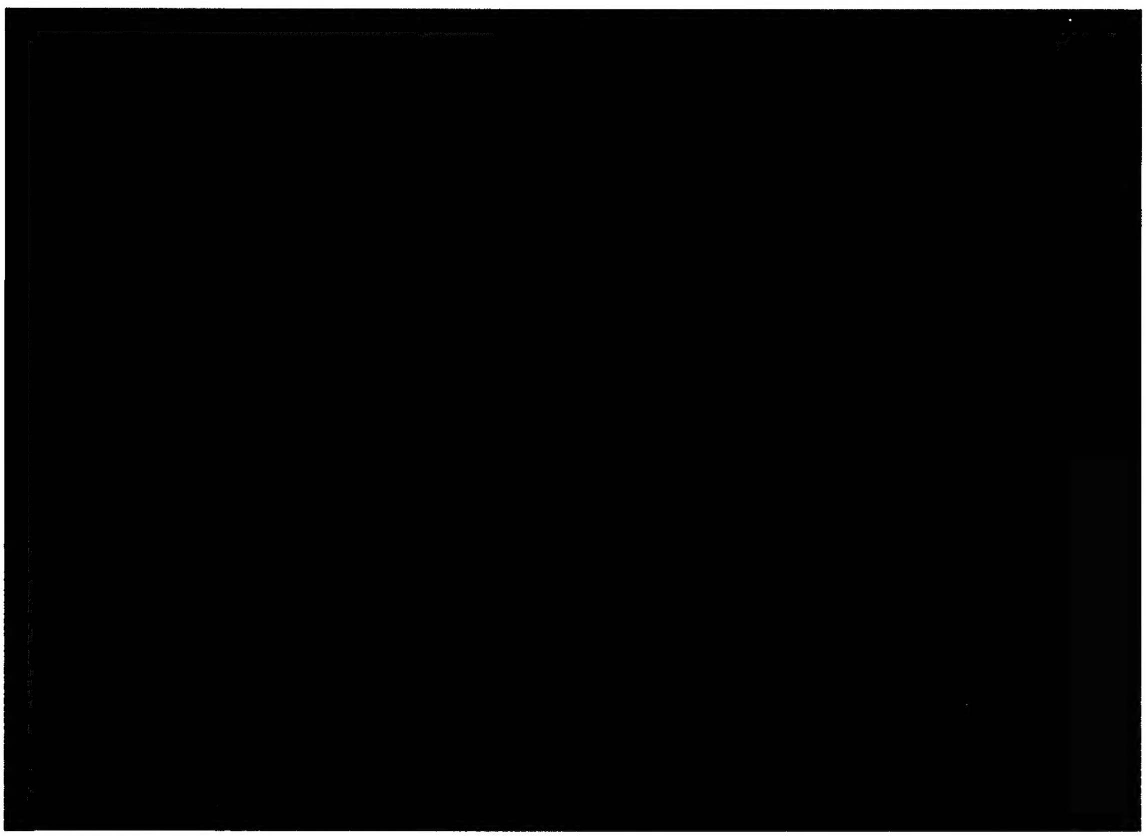

Fig. 5.12 End view of Delta launch vehicle pressure contours.

6. REFERENCES

1. Barth, T.J., "A 3-D Upwind Euler Solver for Unstructured Meshes," AIAA Paper 91-1548, 1991.
2. Batina, J.T., "A Fast Implicit Upwind Solution Algorithm For Three-Dimensional Unstructured Dynamic Meshes," AIAA Paper 92-0447, 1992.
3. Frink, N.T., Parikh, P. and Pirzadeh, S., "Aerodynamic Analysis of Complex Configurations Using Unstructured Grids," AIAA Paper 91-3292, 1991.
4. Jameson, A., Baker, T.J. and Weatherill, N.P., "Calculation of Inviscid Transonic Flow Over a Complete Aircraft," AIAA Paper 86-0103, 1986.
5. Kallinderis, Y., Parthasarathy, V. and Wu, J., "A New Euler Scheme and Adaptive Refinement/Coarsening Algorithm for Tetrahedral Grids," AIAA Paper 92-0446, 1992.
6. Lohner, R. and Baum, J.D., "Numerical Simulation of Shock Interaction with Complex Geometry Three-Dimensional Structures Using a New Adaptive H-Refinement scheme on Unstructured Grids," AIAA Paper 90-0700, 1990.
7. Marcum, D. and Agarwal, R., "A Finite Element Navier-Stokes Solver for Unstructured Grids," AIAA J., Vol. 30., No. 3, p. 648, 1992.
8. Mavriplis, D.J., "Three-Dimensional Unstructured Multigrid for the Euler Equations," AIAA J., Vol. 30, No. 7, p. 1753, 1992.
9. Peraire, J. and Peiro, J., "A 3D Finite Element Multigrid Solver for the Euler Equations," AIAA Paper 92-0449, 1992.
10. Hassan, O., Morgan, K. and Peraire, J., "An Implicit Finite Element Method for High Speed Flows," AIAA Paper 90-0402, 1990.
11. Stoufflet, B., Periaux, J., Fezoui, F. and Dervieux, A., " Numerical Simulations of 3-D Hypersonic Euler Flows Around Space Vehicles Using Adapted Finite Elements," AIAA Paper 87-0560, 1987.
12. Weatherill, N.P., Hassan, O., Marchant, M.J., and Marcum, D.L., "Adaptive Inviscid Flow Solutions for Aerospace Geometries on Efficiently Generated Unstructured Tetrahedral Meshes," AIAA Paper 93-3390, 1993.
13. Weatherill, N.P., Hassan, O., and Marcum, D.L., "Calculation of Steady Compressible Flowfields with the Finite-Element Method," AIAA Paper 93-0341, 1993.
14. Barth, T.J., "Numerical Aspects of Computing Viscous High Reynolds Number Flows on Unstructured Meshes," AIAA Paper 91-0721, 1991.
15. Holmes, D.G. and Connell, S., "Solution of the 2-D Navier-Stokes Equations on Unstructured Adaptive Grids," AIAA Paper 89-1932, 1989.
16. Mavriplis, D.J., "Algebraic Turbulence Modeling for Unstructured and Adaptive Meshes," AIAA J., Vol. 29, No. 12, p. 2086, 1992.
17. Pan, D. and Cheng J.-C., "Upwind Finite-Volume Navier-Stokes Computations on Unstructured Triangular Meshes," AIAA J., Vol. 31, No. 9, p. 1618, 1993.

18. Rostand, P., "Algebraic Turbulence Models for the Computation of Two-Dimensional High-Speed Flows Using Unstructured Grids," Intl. J. Num. Meth. Fluids, Vol. 9, p. 1121, 1989.

19. Nakahashi, K., "Adaptive-Prismatic-Grid Method for External Viscous Flow Computations," AIAA Paper 93-3314, 1993.

20. Chalot, F., Zdenek, J., Mallet, M., Ravachol, M. and Roge, G., "Development of a Finite Element Navier-Stokes Solver with Applications to Turbulent and Hypersonic Flows," AIAA Paper 92-0670, 1992.

21. Marcum, D.L. and Weatherill, N.P., "Finite Element Calculations of Inviscid and Viscous Flow Fields about Launch Vehicle Configurations," VIII International Conference on Finite Elements in Fluids, Barcelona, Spain, 1993.

22. Morgan, K. and Probert, E., "Line Relaxation Methods for the Solution of Two-Dimensional and Three-Dimensional Compressible Flows," AIAA Paper 93-3366, 1993.

23. Simpson, L.B. and Whitfield, D.L., "Flux-Difference Split Algorithm for Unsteady Thin-Layer Navier-Stokes Equations," AIAA Journal, Vol. 30, No. 4, p. 914, 1992.

24. Janus, J.M., Horstman, M., Howard, Z., and Whitfield, D.L., "Unsteady Flowfield Simulation of Ducted Prop-Fan Configurations," AIAA Paper 92-0521, 1992.

25. Marcum, D.L. and Weatherill, N.P., "Unstructured Grid Generation Using Iterative Point Insertion and Local Reconnection," *AIAA Paper 94-1926*, 1994.

26. Marcum, D.L., "Generation of Unstructured Grids for Viscous Flow Applications," *AIAA Paper 95-0212*, 1995.

27. Shepard, M.S. and Georges, M.K., "Automatic Three-Dimensional Mesh Generation by the Finite Octree Technique," *International Journal of Numerical Methods in Engineering*, **32**, 709-749, (1991).

28. Peraire, J., Peiro, J., Formaggia, L., Morgan, K., and Zienkiewicz, O.C., "Finite Element Euler Computations in Three-Dimensions," *International Journal of Numerical Methods in Engineering*, **26**, 2135-2159, (1988).

29. Lohner, R. and Parikh, P., "Three-Dimensional Grid Generation by the Advancing-Front Method," *International Journal of Numerical Methods in Fluids*, **8**, 1135-1149, (1988).

30. Weatherill, N.P., "A Method for Generation of Unstructured Grids Using Dirichlet Tessellations," Princeton University, *MAE Report No. 1715*, 1985.

31. Baker, T.J., "Three-Dimensional Mesh Generation by Triangulation of Arbitrary Point Sets," *AIAA Paper 87-1124*, 1987.

32. Holmes, D.G. and Snyder, D.D., "The Generation of Unstructured Meshes Using Delaunay Triangulation," *Proceedings of the Second International Conference on Numerical Grid Generation in Computational Fluid Dynamics*, Eds. Sengupta, S., Hauser, J. Eisman, P.R., and Thompson, J.F., Pineridge Press Ltd., 1988.

33. George, P.L., Hecht, F., and Saltel, E. "Fully Automatic Mesh Generator for 3D Domains of any Shape," *Impact of Computing in Science and Engineering*, **2**, 187-218, 1990.

34. Roe, P. L., "Approximate Riemann Solvers, Parameter Vectors, and Difference Schemes," *Journal of Computational Physics*, Vol. 43, 1981. pp. 357 – 372.

35. Anderson, W. K., and Bonhaus, D. L., "An Implicit Upwind Algorithm for Computing Turbulent Flows on Unstructured Grids," *Computers Fluids*, Vol. 23, No. 1, 1994. pp. 1 – 21.

36. Barth, T. J., and Jespersen, D. C., "The Design and Application of Upwind Schemes on Unstructured Meshes," AIAA Paper 89–0366, January 1989.

37. Venkatakrishnan, V., "On the Accuracy of Limiters and Convergence to Steady State Solutions," AIAA Paper 93–0880, January 1993.

38. Spalart, P. R., and Allmaras, S. R., "A One Equation Turbulence Model for Aerodynamic Flows," AIAA Paper 92–0439, January 1992.